

# Innermost Stable Circular Orbit of Inspiring Neutron-Star Binaries: Tidal Effects, Post-Newtonian Effects and the Neutron-Star Equation of State

Dong Lai and Alan G. Wiseman

*Theoretical Astrophysics, 130-33, California Institute of Technology  
Pasadena, CA 91125*

E-mail: dong@tapir.caltech.edu; agw@tapir.caltech.edu

(June 29, 2021)

We study how the neutron-star equation of state affects the onset of the dynamical instability in the equations of motion for inspiring neutron-star binaries near coalescence. A combination of relativistic effects and Newtonian tidal effects cause the stars to begin their final, rapid, and dynamically-unstable plunge to merger when the stars are still well separated and the orbital frequency is  $\approx 500$  cycles/sec (*i.e.* the gravitational wave frequency is approximately 1000 Hz). The orbital frequency at which the dynamical instability occurs (*i.e.* the orbital frequency at the innermost stable circular orbit) shows modest sensitivity to the neutron-star equation of state (particularly the mass-radius ratio,  $M/R_o$ , of the stars). This suggests that information about the equation of state of nuclear matter is encoded in the gravitational waves emitted just prior to the merger.

PACS Numbers: 97.80.Fk, 04.25.Dm, 04.40.Dg, 97.60.Jd

## I. INTRODUCTION

Binary neutron star systems which are spiraling toward their final coalescence under the dissipative influence of gravitational radiation reaction forces are the primary targets for detection of gravitational waves by interferometric gravitational wave detectors such as LIGO and VIRGO [1,2]. Extracting the gravitational waves from the detector noise and making use of the information encoded in the signals will require a thorough knowledge of the expected waveforms produced by these binaries [2,3]. In this paper we explore the effect of the neutron-star equation of state on the orbital evolution and gravitational wave emission of binaries just prior to merging. Specifically, we show that a combination of post-Newtonian (relativistic) effects and Newtonian tidal effects (which depend on the equation of state) conspire to induce a dynamical instability in the orbital motion, which causes the plunge to final coalescence to begin somewhat sooner – and to proceed somewhat faster – than it would simply under the influence of the dissipative radiation reaction force. Thus the motion of the bodies during the late stages of binary inspiral depends on the structure of the neutron stars. Consequently, the

gravitational waveform emitted during this short portion of the final coalescence will be imprinted with information about the nuclear equation of state.

During the final  $\sim 10$  minutes or the last  $\sim 8000$  orbits of a neutron star binary inspiral, the orbital frequency increases from about 5 Hz on up to a cutoff of a few hundreds to a thousand Hertz (roughly corresponding to the orbital frequency when the final plunge begins). Thus the gravitational wave frequency (twice the orbital frequency for the dominant quadrupole radiation) *chirps* through the LIGO detector bandwidth during this period [1]. The evolution of the binary in these last few minutes of the inspiral is very sensitive to a number of relativistic effects, such as gravitational-wave tails and spin-orbit coupling (dragging of inertial frames). The gravitational waveform emitted by the binary in this portion of the coalescence, the adiabatic inspiral, is currently being extensively studied [4–6]. During most of this inspiral phase the neutron stars can be treated as simple point masses because the effects associated with the finite stellar size turn out to be small: (i) The neutron star has too small a viscosity to allow for angular momentum transfer from the orbit to the stellar spin via viscous tidal torque [7,8]; (ii) The effect of the spin-induced quadrupole is negligible unless the neutron star has rotation rate close to the break-up limit [7,10]; (iii) Resonant excitations of neutron star internal modes (which occur at orbital frequencies less than 100 Hz) produce only a small change in the orbital phase due to the weak coupling between the modes and the tidal potential [11–13]; (iv) The correction to the equation of motion from the (static) tidal interaction is of order  $(R_o/r)^5$  (where  $R_o$  is the neutron star radius,  $r$  is the orbital separation [14]), which is negligible except when  $r$  is smaller than a few stellar radii. Since  $R_o \simeq 5M$  for a typical neutron star of mass  $1.4M_\odot$  and radius 10 km, the tidal effect is essentially a (post)<sup>5</sup>-Newtonian correction [9]. The expression for the phase error induced by the tidal effect is given in Ref. [10]. The fact that the evolution of the binary system as it sweeps through the low frequency band of the detector is insensitive to finite-size effects means that the measurement of the inspiral waveform will allow us to probe cleanly into the intricate structure of general relativity, and to test whether general relativity is the correct theory of gravity [15,16]. Moreover, some of the parameters of the binary system, such as the masses of the stars, can be

determined with reasonable accuracy [17,18]. However, the waveform’s lack of dependence on the finite size of the objects during the most of the adiabatic inspiral also implies that information about the internal structure of the neutron star is only imprinted on the radiation emitted just prior to coalescence when the orbital radius is small.

Indeed at small orbital separations, tidal effects are expected to be very important. In a purely *Newtonian* analysis, the interaction potential between star  $M'$  and the tide-induced quadrupole of  $M$ ,  $V_{tide} \sim -M'^2 R_o^5 / r^6$ , increases with decreasing  $r$ . The potential becomes so steep that a dynamical instability develops, accelerating the coalescence at small orbital radius. This Newtonian instability has been fully explored using semi-analytic models in Ref. [10] and Ref. [19] (hereafter referred to as LS). It has also been examined numerically in Refs. [20,21].

However, a purely Newtonian treatment of the binary at small separation is clearly not adequate, as general relativistic effects will also be important in this regime; and general relativistic effects can also make the orbit unstable. For example, a test particle in circular orbit around a Schwarzschild black hole will experience an “innermost stable circular orbit” at  $r_{\text{isco}} = 6M$  (or  $5M$  in harmonic coordinates). This unstable behavior is caused by higher-order relativistic corrections included in the Schwarzschild geodesic equations of motion. For computing the orbital evolution of two neutron stars of comparable mass near coalescence, the test-mass limit is obviously inadequate. In order to explore the orbital instability for such systems, Kidder, Will and Wiseman [22] (hereafter referred as KWW) developed *hybrid* equations of motion. These equations augment the the Schwarzschild geodesic equations of motion with the finite-mass terms of the (post)<sup>5/2</sup>-Newtonian equations of motion. Including these finite mass terms in the equation of motion moved the innermost-stable-circular-orbit radius farther out (in units of the total mass).<sup>1</sup> In this paper, we augment the hybrid equations with contributions due to the tidal deformation of the stars. In a nutshell, the work presented here combines the Newtonian tidal analysis of LS [19] with the relativistic point-mass analysis of KWW [22] to yield a more complete picture of the neutron-star coalescence prior to merging.

We note, that unlike a test-particle around a Schwarzschild black hole, the very notion of “innermost stable circular orbit” is poorly defined for objects of comparable mass. After all, in the relativistic regime the binary orbit will be decaying rapidly due to radiation reac-

tion; thus the orbit is not circular, but rather a decaying spiral. In order to give a semi-quantitative definition of “innermost stable circular orbit” we use the artifice of “shutting off” all the dissipative terms in the equation of motion and looking for the point where the solutions of the remaining non-dissipative equations become dynamically unstable. The use of hybrid equations of motion augmented with the tidal terms allows us to map out the dependence of the critical radius  $r_{\text{isco}}$ , or the corresponding orbital frequency  $f_{\text{isco}}$ , for a wide range of allowed neutron star equations of state (parametrized by radius and effective polytropic index; see Figure 1). We believe that clearing up such dependence is important, and this analysis provides a benchmark with which comparisons can be made with future numerical results. *Indeed, an important point we wish to make in this paper is that neither relativistic (post Newtonian) effects nor Newtonian tidal effects can be neglected near the instability limit, and the critical frequency can be much lower than the value obtained when only one of these effects are included.*

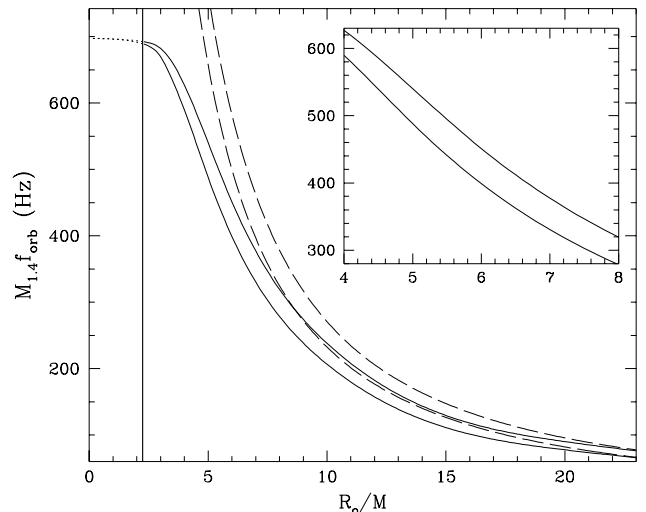


FIG. 1. The critical orbital frequency (at the inner-most stable orbit) as a function of the ratio of the neutron star radius  $R_o$  and mass  $M$ . The solid curves show the results including both relativistic and tidal effects (the lower curve is for  $\Gamma = 3$  while the upper one is for  $\Gamma = 2$ ), the dashed curves are the Newtonian limit given by Eqs. (8)-(9). The vertical line corresponds to  $R_o/M = 9/4$ , the minimum value for any physical neutron star. The insert is a close-up for the nominal range of  $R_o/M = 4 - 8$  as given by all the available nuclear EOS’s. Two curves within the insert should bracket all the physical values of  $f_{\text{isco}}$ .

The main results of our analysis are summarized in Figure 2 and 3. Figure 2 shows that the rate of radial infall for stars near coalescence is substantially underestimated if one models the coalescence as a Newtonian circular-orbit decaying solely under the influence of radiation reaction (top dotted curve). In other words, the rate of coordinate infall is substantially enhanced by the

<sup>1</sup>See Wex and Schäfer [23] for a critique and an alternative construction. Their post-Newtonian calculation suggests that the innermost stable orbit may occur at an even greater separation.

non-dissipative terms. Somewhat more relevant for observational purposes, Figure 3 shows that the number of orbits (or gravitational wave cycles) per logarithmic frequency interval is substantially reduced by the unstable collapse of the orbit. Both plots show modest sensitivity to the equation of state.

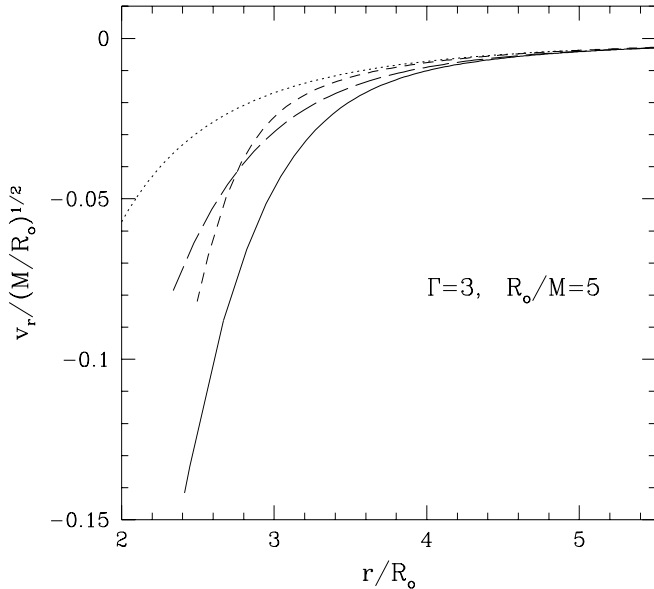


FIG. 2. The radial infall coordinate velocity during binary coalescence, with  $M = M' = 1.4M_\odot$ ,  $R_o/M = 5$ ,  $\Gamma = 3$ , all calculated using 2.5PN radiation reaction. The solid line is the result including relativistic and tidal effects, the short-dashed line includes only tidal effects, the long-dashed line includes only relativistic effects. The dotted line is the point mass “Newtonian” result.

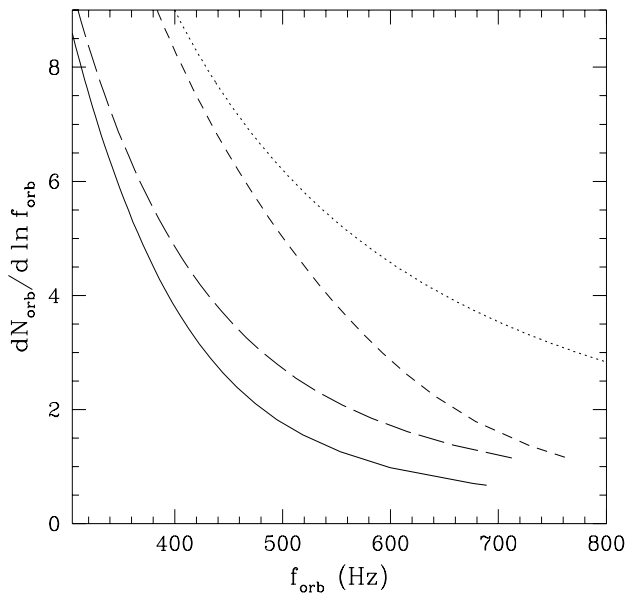


FIG. 3. The number of orbits the binary spends per logarithmic frequency. The labels are the same as in Fig. 2.

The remainder of the paper is organized as follows: In section II we present our equations of motion. In section III we examine the orbital stability using the non-dissipative portion of the equations of motion, and thus identify the location of the “innermost stable circular orbit”. In section IV we include the dissipative terms that were omitted in the analysis of section III, and evolve the full equations of motion. In section V we briefly discuss the relevance of our results to numerical hydrodynamic calculations and to gravitational wave signal analysis.

## II. EQUATIONS OF MOTION INCLUDING TIDAL AND GENERAL RELATIVISTIC EFFECTS

Consider a binary containing two neutron stars of mass  $M$  and  $M'$ , each obeying a polytropic equation of state  $P = K\rho^\Gamma$ . We use the compressible ellipsoid model for binary stars developed in LS [19]. Basically, we model the tidally deformed neutron star as an ellipsoid, with internal density profile similar to that of a spherical polytrope. The dynamics of such a neutron star (so called Riemann-S ellipsoid) is characterized by the three principal axes ( $a_1, a_2, a_3$  for star  $M$  and  $a'_1, a'_2, a'_3$  for star  $M'$ ), the angular velocity ( $\Omega$  and  $\Omega'$ ) of the ellipsoidal figure about a principal axis (perpendicular to the orbital plane) and the internal motion of the fluid with uniform vorticity. The non-zero internal fluid motion is necessary because the binary neutron stars are not expected to corotate with the orbit due to rapid orbital decay and small viscosity [7,8]. Although the Newtonian tidal interaction between the neutron stars can be treated exactly in the linear regime using mode decomposition [11], the ellipsoid model has the advantage that it can be extended to the nonlinear regime at small orbital radii, when the tidal deformation of the star becomes significant.

The Newtonian dynamical equations for the binary neutron stars as derived in LS include the familiar Newtonian ( $1/r^2$ ) force-law for point-masses orbiting one another; they further contain Newtonian terms involving finite size (tidal) effects. A post-Newtonian treatment of the tidal problem would give the relativistic corrections to these terms, namely the standard point-mass, post-Newtonian corrections to the equations of motion, as well as relativistic corrections to the quadrupole moment and corrections due to higher moments the bodies. (See Appendix F of [24].) To insure that our equations of motion at least agree with the known post-Newtonian, point-mass equations we augment these Newtonian equations of motion with the hybrid equations of KWW. However, we use only the Newtonian equations to describe the evolution of the neutron stars structure ( $a_i$  and  $a'_i$ ) and the fluid motion (the figure rotation rate and the internal vorticity) within the stars. These are given by Eqs. (2.18)-(2.22) of LS. In other words, we neglect the relativistic corrections to the fluid motion, self-gravity and tidal interaction. These corrections are secondary

effects and should not modify the *orbital dynamics* appreciably (e.g., the Newtonian tidal interaction between the two stars scales approximately as  $M^2 R_o^5/r^6$ , and its relativistic correction is of order  $M/r$  smaller). As noted before, the tidal interaction enters the Newtonian potential as a correction of  $O[(R_o/r)^5] \sim O[(M_t/r)^5]$ , in effect, as a (post)<sup>5</sup>-Newtonian term. Therefore, by not including relativistic corrections to these tidal terms, we are merely omitting terms which are of (post)<sup>6</sup>-Newtonian order. In fact, the largest error comes from neglecting the post-Newtonian correction (of order  $M/R_o$ ) to the internal stellar structure (see Sec. III.B for an estimate of its effect on  $f_{\text{isco}}$ ). The relativistic corrections to the orbital motion, however, are very important. Our equations of orbital motion can be assembled from Eqs. (2.23)-(2.24) of LS and from Eqs. (1.2)-(1.3) of KWW:

$$\begin{aligned} \ddot{r} = & r\dot{\theta}^2 - \frac{M_t}{r^2}(A_H + B_H\dot{r}) \\ & - \frac{3\kappa_n}{10} \frac{M_t}{r^4} [a_1^2(3\cos^2\alpha - 1) + a_2^2(3\sin^2\alpha - 1) - a_3^2] \\ & - \frac{3\kappa'_n}{10} \frac{M_t}{r^4} [a_1'^2(3\cos^2\alpha' - 1) + a_2'^2(3\sin^2\alpha' - 1) - a_3'^2] \\ & - \frac{M_t}{r^2}(A_{5/2} + B_{5/2}\dot{r}) - \frac{32}{5}r[\Omega^5(I_{11} - I_{22})\sin 2\alpha \\ & + \Omega'^5(I'_{11} - I'_{22})\sin 2\alpha'], \end{aligned} \quad (1)$$

$$\begin{aligned} \ddot{\theta} = & -\frac{2\dot{r}\dot{\theta}}{r} - \frac{M_t}{r^2}B_H\dot{\theta} \\ & - \frac{3\kappa_n}{10} \frac{M_t}{r^5}(a_1^2 - a_2^2)\sin 2\alpha - \frac{3\kappa'_n}{10} \frac{M_t}{r^5}(a_1'^2 - a_2'^2)\sin 2\alpha' \\ & - \frac{M_t}{r^2}B_{5/2}\dot{\theta} - \frac{32}{5}[\Omega^5(I_{11} - I_{22})\cos 2\alpha \\ & + \Omega'^5(I'_{11} - I'_{22})\cos 2\alpha'], \end{aligned} \quad (2)$$

where  $M_t = M + M'$  is the total mass,  $\alpha$  ( $\alpha'$ ) is the misalignment angle between the tidal bulge of  $M$  ( $M'$ ) and the line joining the two masses,  $\kappa_n, \kappa'_n$  are dimensionless structure constants depending on the mass concentration within the stars. In Eqs. (1) and (2) the last two lines contain the ‘‘dissipative’’ terms due to gravitational radiation reaction. The quantities  $A_H, B_H, A_{5/2}, B_{5/2}$ , which include the ‘‘hybrid’’ corrections to the equation of motion, are given by

$$\begin{aligned} A_H = & \frac{1 - M_t/r}{(1 + M_t/r)^3} - \left[ \frac{2 - M_t/r}{1 - (M_t/r)^2} \right] \frac{M_t}{r} \dot{r}^2 + v^2 \\ & - \eta \left( 2\frac{M_t}{r} - 3v^2 + \frac{3}{2}\dot{r}^2 \right) + \eta \left[ \frac{87}{4} \left( \frac{M_t}{r} \right)^2 \right. \\ & \left. + (3 - 4\eta)v^4 + \frac{15}{8}(1 - 3\eta)\dot{r}^4 - \frac{3}{2}(3 - 4\eta)v^2\dot{r}^2 \right. \\ & \left. - \frac{1}{2}(13 - 4\eta)\frac{M_t}{r}v^2 - (25 + 2\eta)\frac{M_t}{r}\dot{r}^2 \right] \end{aligned} \quad (3)$$

$$\begin{aligned} B_H = & - \left[ \frac{4 - 2M_t/r}{1 - (M_t/r)^2} \right] \dot{r} + 2\eta\dot{r} - \frac{1}{2}\eta\dot{r} \left[ (15 + 4\eta)v^2 \right. \\ & \left. - (41 + 8\eta)\frac{M_t}{r} - 3(3 + 2\eta)\dot{r}^2 \right], \end{aligned} \quad (4)$$

$$A_{5/2} = -\frac{8}{5}\eta\frac{M_t}{r}\dot{r} \left( 18v^2 + \frac{2}{3}\frac{M_t}{r} - 25\dot{r}^2 \right), \quad (5)$$

$$B_{5/2} = \frac{8}{5}\eta\frac{M_t}{r} \left( 6v^2 - 2\frac{M_t}{r} - 15\dot{r}^2 \right), \quad (6)$$

where  $v^2 = \dot{r}^2 + r^2\dot{\theta}^2$ ,  $\eta = \mu/M_t$  and  $\mu = MM'/M_t$ . Also the multipole moments can be expressed as

$$I_{ii} = \kappa_n M a_i^2/5, \quad I'_{ii} = \kappa'_n M' a_i'^2/5. \quad (7)$$

Note that in Eqs. (1)-(2), we have also included the leading order radiation reaction forces due to tidal deformation.

Admittedly, this is not a consistent post-Newtonian expansion of the true equations of motion; however it is correct in several important limiting cases: (i) In the limit that  $a_i \rightarrow 0$  and  $a'_i \rightarrow 0$  and the limit  $\eta \rightarrow 0$ , we recover the *exact* Schwarzschild equation of motion. (ii) In the point-mass limit ( $a_i \rightarrow 0$  and  $a'_i \rightarrow 0$ ) we recover the hybrid equations given in KWW. KWW presented an argument that suggested that the higher-order,  $\eta$ -dependent, (post)<sup>3</sup>-Newtonian – as yet uncalculated – corrections to these equations have only a modest effect on the equations of motion. See Figure 6 of Ref. [22]. However, until these terms are calculated it is unclear just how large an effect they will have on the location of the innermost stable orbit. (iii) In the non-relativistic limit we recover the equations of motion given in LS. These equations contain the dominant contributions to the equations of motion due to the finite sizes of the objects.

Note that although Eqs. (1) and (2) make reference to the orbital radius  $r$ , we are always aware that this is a gauge dependent quantity and of little meaning for a distant observer. Observationally, the more meaningful quantity is the orbital frequency as measured by distant observers, and we shall use frequency rather the radius in presenting most of our results.

### III. INSTABILITY OF THE NON-DISSIPATIVE EQUATIONS OF MOTION

#### A. Method to Determine the Stability Limit

We now form a set of non-dissipative equations of motion, by simply discarding the gravitational radiation reaction terms given in the last two lines of Eq. (1) and Eq. (2). These non-dissipative dynamical equations admit equilibrium solutions, which are obtained by setting  $\dot{r} = \ddot{r} = \dot{\theta} = \ddot{\theta} = \dot{\Omega}_{orb} = \alpha = \alpha' = 0$  as well as  $\dot{a}_i = \dot{a}'_i = 0$ . For a given  $r$ , the evolution equations for the neutron star structure reduce to a set of algebraic equations for  $a_i$  and  $a'_i$ , while the orbital equation (2) gives the orbital frequency  $\Omega_{orb}$ . These equations are solved using a Newton-Raphson method, yielding an equilibrium binary model. Thus a sequence of binary models parametrized by  $r$  can be constructed.

To determine the stability of the orbit of a binary model, we simply use the equilibrium parameters as initial conditions for our non-dissipative equations of motion. We add a small perturbation to the equilibrium model and let the system evolve. In this way we locate the critical point of the dynamical equations, corresponding to the dynamical stability limit of the equilibrium binary or the inner-most stable circular orbit: for  $r > r_{\text{isco}}$ , the binary is stable, and the system oscillates with small amplitude about the initial configuration; for  $r < r_{\text{isco}}$ , the binary is unstable, and the perturbation grows, leading to the swift merger of the neutron stars even in the absence of dissipation.

## B. Results

For concreteness, we present results only for binary neutron stars with equal masses ( $M = M'$ ), both having zero spin at large orbital separation, although our equations are adequate to treat the most general cases [19].

The polytropic relation  $P = K\rho^\Gamma$  provides a useful parametrization to the most general realistic nuclear equation of state (EOS). Since the radius  $R_o$  of the non-rotating neutron star of mass  $M$  is uniquely determined by  $K$  and  $\Gamma$ , we can alternatively use  $R_o/M$  and  $\Gamma$  to characterize the EOS. For a canonical neutron star with mass  $M = 1.4M_\odot$ , all EOS tabulated in [25] give  $R_o/M$  in the range of 4 – 8, while modern microscopic nuclear calculations typically give  $R_o/M = 5$  [26]. For a given  $R_o/M$ , the polytropic index  $\Gamma$  specifies the mass concentration within the star. Except for extreme neutron star masses ( $M \lesssim 0.5M_\odot$  or  $M \gtrsim 1.8M_\odot$ ) typical values of  $\Gamma$  lie in the range of  $\Gamma = 2 - 3$  [10].

In Table I, we list the physical properties of the equilibrium binary neutron stars at the dynamical stability limit for several values of  $R_o/M$  and  $\Gamma = 3$ . In Figure 1, the orbital frequency  $f_{\text{isco}}$  is shown as a function of  $R_o/M$  for  $\Gamma = 2$  and  $\Gamma = 3$ . Clearly, in the limit of  $R_o/M \rightarrow 0$ ,  $f_{\text{isco}}$  approaches the point mass result  $f_{\text{isco}} = 697M_{1.4}^{-1}$  Hz obtained in KWW<sup>2</sup>. In the non-relativistic limit we recover the pure Newtonian result [10,19]:

$$\begin{aligned} f_{\text{isco}} &= 657M_{1.4}^{-1}(5M/R_o)^{3/2} \text{ (Hz)} & (\Gamma = 3), & (8) \\ f_{\text{isco}} &= 766M_{1.4}^{-1}(5M/R_o)^{3/2} \text{ (Hz)} & (\Gamma = 2). & (9) \end{aligned}$$

*For typical neutron star radius  $R_o/M = 5$ , the critical frequency ranges from 488 Hz (for  $\Gamma = 3$ ) to 540 Hz (for  $\Gamma = 2$ ), while both the pure Newtonian (with tides) calculation and the pure point-mass hybrid calculation give a result 30 – 40% larger.* There are two physical causes

for the reduction in  $f_{\text{isco}}$ : (i) The binary becomes unstable at larger orbital separation due to the steepening of the interaction potential from both tidal and relativistic effects; (ii) For a given orbital radius (itself a gauge dependent quantity), the post-Newtonian orbital frequency as measured by an observer at infinity is smaller than the Newtonian orbital frequency<sup>3</sup>. We conclude that to neglect either the tidal effects or the relativistic effects can lead to large error in the estimated critical frequency.

Except for the intrinsic uncertainties associated with the hybrid equations of motion [22,23], the main uncertainty in our determination of  $f_{\text{isco}}$  comes from neglecting post-Newtonian corrections to (i) the stellar structure and (ii) the tidal potential. The first correction *decreases* the tide-induced quadrupole; the fractional change is of order  $-M/R_o$ . The second *increases* the quadrupole by a fraction of order  $M'/r$ . We can estimate how much  $f_{\text{isco}}$  is modified by these two corrections. In Newtonian theory,  $r_{\text{isco}}$  is approximately determined by the condition  $MM'/r \sim M'^2R_o^5/r^6$ . Including the relativistic corrections this condition becomes  $MM'/r \sim M'^2R_o^5/r^6(1 - \delta)$ , where  $\delta \sim [O(M/R_o) - O(M'/r)] \lesssim 20\%$ . Thus the change in  $f_{\text{isco}}$  due to these two effects is  $\Delta f_{\text{isco}}/f_{\text{isco}} \simeq 0.3\delta \lesssim 6\%$ , i.e., the critical frequency increases by a few percent [27].

As emphasized in Sec. I, the critical radius (or critical frequency), at which the non-dissipative equations become dynamically unstable, is meaningful only in the sense that when  $r < r_{\text{isco}}$ , the binary will coalesce on dynamical (orbital) timescale even in the absence of dissipation. In the realistic situation, the dissipative radiation reaction forces will also be rapidly driving the binary to coalescence. Therefore to determine the significance of the dynamical instability we must compute the orbital evolution with the full equations of motion – including the radiation reaction.

## IV. ORBITAL EVOLUTION PRIOR TO MERGER

We now include the dissipative radiation reaction forces in our analysis. In this case the plunge will be driven by both the dissipative, as well as the non-dissipative effects associated with the steepening potential (both the tidal potential and the relativistic potential). But what effect is dominant? In order to numerically investigate this question, we choose a specific system with  $M = M' = 1.4M_\odot$ ,  $R_o/M = 5$  and  $\Gamma = 3$ . The orbital evolution begins when the stars are well outside the innermost stable circular orbit limit. We consider four different inspiral scenarios. (i) A purely dissipative inspiral: a system of point masses subject only to

<sup>2</sup>KWW [22] give a correct expression for  $r_{\text{isco}}/M_t$ , but incorrectly give  $f_{\text{isco}}=710$  Hz due to a numerical error.

<sup>3</sup>In the case of equal masses, at first post-Newtonian order  $\Omega_{\text{orb}} = \Omega_{\text{Kepler}}[1 - (11/8)(M_t/r)]$ . See Ref. [4].

a Newtonian ( $1/r^2$ ) force and (post)<sup>5/2</sup>-Newtonian radiation reaction force. In this case the infall rate is given by  $v_r = \dot{r} = -(64/5)\eta(M_t/r)^3$ . [Specifically, we set  $A_H = 1$  and  $B_H = a_i = a'_i = I_{kk} = I'_{kk} = 0$  in Eqs. (1)-(2).] This is depicted by the dotted curve in Figure 2 and 3. (ii) A purely relativistic plunge in which we neglect the tidal effects [Specifically we set  $a_i = a'_i = I_{kk} = I'_{kk} = 0$  in Eqs. (1)-(2)]. This relativistic case is depicted by the long-dashed curve in Figure 2 and 3. (iii) A tidally enhanced plunge: we include only the Newtonian terms in Eqs. (1)-(2) and the radiation reaction force. [Specifically we set  $A_H = 1$  and  $B_H = 0$  in Eqs. (1)-(2).] This case is depicted by the short-dashed curve in Figure 2 and 3. (iv) Finally, we evolve the complete dynamical equations including all terms in Eqs. (1)-(2); this is depicted by the solid curve in Figure 2 and 3. Each integration is terminated when the surfaces of the stars touch, i.e., at  $r \simeq 2a_1$  (for the point-mass problem, the calculation is terminated at  $r \simeq 2R_o$ ).

In Figure 2 we clearly see that the non-dissipative effects – tidal and relativistic – substantially increase the rate of infall. The radial velocity at binary contact is comparable to the tangential velocity. We also note that the radial coordinate velocity is a gauge dependent quantity; therefore our only intent in using it in Figure 2 is to convey the general trend that the rate of infall is enhanced by the dynamical instability.

Figure 3 shows the number of orbits the binary spends per logarithmic frequency. In the simplest point-mass, Newtonian-plus-radiation-reaction case [case (i) above], the result can be calculated analytically

$$\begin{aligned} dN_{orb}/d \ln f_{orb} &= (5/192\pi)\mu^{-1}M_t^{-2/3}(2\pi f_{orb})^{-5/3} \\ &= 1.95 \times 10^5 (M_{1.4} f_{orb}/\text{Hz})^{-5/3}, \end{aligned} \quad (10)$$

which gives 6 cycles at  $f_{gw} \simeq 2f_{orb} = 1000$  Hz. In contrast, the tidal and relativistic effects reduce this number to less than 2.

Figure 4 shows the wave energy emitted around a given frequency,  $dE_{gw}/d \ln f_{orb} = (\Omega_{orb}/\dot{\Omega}_{orb})\dot{E}_{gw}$ , where  $\dot{E}_{gw}$  is calculated using the simple quadrupole radiation formula. The Newtonian plus radiation reaction result is  $dE_{gw}/d \ln f_{orb} = 1.63 \times 10^{-3}(f_{orb}/\text{Hz})^{2/3}M^2/R_o$ . We see that the radiation power near contact becomes much smaller. Note that  $dE_{gw}/d \ln f_{orb}$  calculated in this way is not exactly the energy power spectrum, which must be obtained from the Fourier transform of the waveform [28]; however, it does provide a semi-quantitative feature of the full analysis; in particular, the dip in the  $dE_{gw}/d \ln f_{orb}$  curve around 600 Hz results from the dynamical instability of the orbit (see also Refs. [21,29], although the calculations presented there are purely Newtonian).

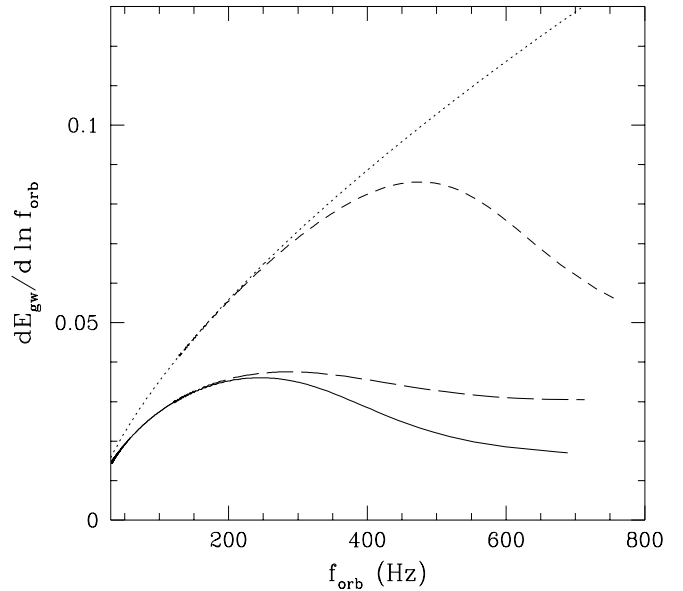


FIG. 4. The quadrupolar gravitational energy emitted near a given frequency. The labels are the same as in Fig. 2.

## V. DISCUSSION

A number of authors have tried to define and locate the innermost stable circular orbit for relativistic coalescing systems of comparable masses [23,30–33] in order to characterize the final moments of a binary coalescence (See [34] for a discussion). The results of the various analyses are not converging to an agreed answer. Obviously, the precise nature of the final coalescence of two neutron stars will only be determined by a numerical simulation using full general-relativistic hydrodynamics. However, the present analysis does point to two interesting features to look for in a full numerical treatment: (i) To get even a qualitative picture of the coalescence, it is necessary to begin the numerical evolution when the stars are still well separated, *i.e.* before the onset of the orbital dynamical instability. The instability – the plunge – causes the coalescence to proceed much more swiftly than a coalescence driven solely by radiation reaction; thus the actual coalescence may differ qualitatively from one computed with a simple radiation-reaction driven inspiral. The final coalescence may be more of a splat, than the slow winding together of the stars [35]. (ii) The instability results from both the tidal effects and the relativistic corrections in the equations of motion. KWW showed that there is no instability in the *first* post-Newtonian relativistic equations of motion; the instability does not show up until at least second post-Newtonian order. Therefore, in order for numerical simulations to see the effects of the relativistic unstable plunge, it will probably require the use of at least second-order, post-Newtonian hydrodynamic code. KWW also showed that the location of the dynamic instability does not converge very rapidly as one

increases the post-Newtonian order of the approximation. [This fact led KWW to the introduce the hybrid equations of motion.] Thus, to get even a qualitatively accurate evolution of the binary near coalescence, it may be necessary to use a full general relativistic hydrodynamic treatment of the coalescence problem, and begin the evolution when the stars are still well separated.

As we have shown, the dynamical instability in the equation of motion will, in effect, cut off the chirping waveform. The frequency of the cut-off is somewhat dependent on the neutron star equation of state. Only in this late stage of the evolution does the equation of state leave a tell-tale sign in the emitted waveform. However, devising a strategy to dig this information from the detector output requires further consideration. Most detection/measurement strategies for coalescing binaries involve integrating template waveforms against long stretches (8000 orbits!) of raw output data, the idea being that one can detect/measure a relatively low amplitude signal by integrating for a long time. Looking for the signature of this very late stage plunge is precisely the opposite: we are looking at the waveform just before coalescence when the amplitude is fairly strong, but the plunge is of fairly short in duration. So answering questions about the plunge (such as, at what orbital frequency did it begin?) requires measuring a relatively large amplitude, but short-duration, effect. Clearly, analysis of such events will require a different detection strategy [28].

## ACKNOWLEDGMENTS

We thank Kip Thorne for useful discussions. This work has been supported by NSF Grants AST-9417371, PHY-9424337 and NASA Grant NAGW-2756 to Caltech. DL also acknowledges support of the Richard C. Tolman Fellowship at Caltech.

---

[1] A. Abramovici, et al., *Science*, **256**, 325 (1992).

[2] K. S. Thorne, in “Proceedings of Snowmass 94 Summer Study on Particle and Nuclear Astrophys. and Cosmology”, eds. E. W. Kolb and R. Peccei (World Scientific, Singapore, 1995).

[3] C. Cutler, et al. *Phys. Rev. Lett.* **70**, 2984 (1993).

[4] L. Blanchet, T. Damour, B. R. Iyer, C. M. Will and A. G. Wiseman, *Phys. Rev. Lett.*, **74**, 3515 (1995).

[5] L. Blanchet, B. R. Iyer, C. M. Will, and A. G. Wiseman, *Class. Quantum Grav.*, in press.

[6] C. M. Will, and A. G. Wiseman, *Phys. Rev. D* (submitted).

[7] L. Bildsten and C. Cutler, *Astrophys. J.* **400**, 175 (1992).

[8] C. S. Kochanek, *Astrophys. J.* **398**, 234 (1992).

[9] Assigning such a high “post-Newtonian” relativistic order to this “Newtonian” tidal effect may seem strange, but the argument goes as follows: The quadrupole correction enters the the Newtonian potential as  $(MM'/r)[1 + Q(R_{equatorial}/r)^2 P_2(\cos\theta)]$ , here the leading term is just the usual  $(1/r)$ -part of the Newtonian Potential,  $Q$  is some measure of the bodies quadrupole moment,  $P_2$  is the second Legendre polynomial. For a typical neutron star  $R_{equatorial} \sim 5M$ , so we might expect the correction term to scale as an  $O[(M/r)^2]$  correction to the Newtonian potential, *i.e.* a (post)<sup>2</sup>-Newtonian correction. However,  $Q$ , the tidally-induced quadrupole moment, also scales as  $(M/r)^3$ . Therefore the quadrupole correction term scales as an  $O[(M/r)^5]$  correction to the Newtonian potential, thus it can be compared to a (post)<sup>5</sup>-Newtonian term.

[10] D. Lai, F. A. Rasio and S. L. Shapiro, *Astrophys. J.*, **420**, 811 (1994).

[11] D. Lai, *Mon. Not. Royal Astro. Soc.* **270**, 611 (1994).

[12] A. Reisenegger and P. Goldreich, *Astrophys. J.* **426**, 688 (1994).

[13] M. Shibata, *Prog. Theor. Phys.* **91**, 871 (1994).

[14] We adopt units in which  $G = c = 1$ . We use the following notation to describe our binary system: The two neutron stars have (comparable) masses  $M$  and  $M'$ , the total mass of the system is denoted  $M_t$ ; Small  $r$  will denote orbital (center to center) coordinate separation; capital  $R_o$  will denote the neutron star radius at large  $r$ .

[15] L. Blanchet and B. S. Sathyaprakash, *Class. Quantum Grav.* **11**, 2807 (1994).

[16] C.M. Will, *Phys. Rev. D* **50**, 6058 (1994).

[17] L. S. Finn and D. F. Chernoff, *Phys. Rev. D.* **47**, 2198 (1993).

[18] C. Cutler and E. Flanagan, *Phys. Rev. D.* **49**, 2658 (1994).

[19] D. Lai and S. L. Shapiro, *Astrophys. J.* **443**, 705 (1995) (LS).

[20] F. A. Rasio and S. L. Shapiro, *Astrophys. J.*, **401**, 226 (1992). *ibid.*, **432**, 242 (1994). Note that these calculations assume (unrealistic) synchronized neutron star rotation. The turning point in the equilibrium energy curve of a corotating binary corresponds to the *secular* instability limit, rather than the dynamical instability limit (see Ref. [10]).

[21] X. Zhuge, J. M. Centrella, S. L. W. Mcmillan, *Phys. Rev. D.* **50**, 6247 (1994).

[22] L. E. Kidder, C. M. Will and A. G. Wiseman, *Phys. Rev. D* **47**, 3281 (1993) (KWW).

[23] N. Wex and G. Schäfer, *Class. Quantum Gravity*, **10**, 2729 (1993).

[24] C. M. Will and A. G. Wiseman, *Phys. Rev. D* (Submitted).

[25] W. D. Arnett and R. L. Bowyer, *Astrophys. J. Suppl.* **33**, 415 (1977).

[26] R. B. Wiringa, V. Fiks and A. Fabrocini, *Phys. Rev. C* **38**, 1010 (1988); for a recent review, see G. Baym, in *Isolated Pulsars*, ed. K. Van Riper, R. Epstein and C. Ho (Cambridge Univ. Press, 1991).

[27] The fact that post-Newtonian effects decrease the tidal distortion is consistent with the finding in Ref. [30] and in M. Shibata (1996, Osaka Univ. Preprint) (whose calcula-

tions assume synchronized neutron star rotation). However, the accuracy of the stability limit given in Ref. [30] is not without question, since the method has been shown to give unphysical result regarding the stability of the neutron star against radial collapse (D. Lai, 1996, Phys. Rev. Lett., in Press).

- [28] D. Kennefick, D. Laurence and K. S. Thorne, Phys. Rev. D., to be submitted (1996).
- [29] M. Ruffert, H.-T. Janka and G. Schäfer, Astro. Astrophys., in press (1996).
- [30] J. R. Wilson and G. J. Mathews, Phys. Rev. Lett. **75**, 4161 (1995); J. R. Wilson, G. J. Mathews and P. Maronetti, Phys. Rev. D., submitted (1996).
- [31] J.P.A. Clark, and D.M. Eardley, Astrophys. J. **215**, 311 (1977).
- [32] J.K. Blackburn and S. Detweiler, Phys. Rev. D. **46**, 2318 (1992).
- [33] G.B. Cook, Phys Rev. D **50**, 5015 (1994).
- [34] D.M. Eardley and E. W. Hirschmann, Preprint gr-qc/9601019.
- [35] See, e.g., M. Shibata, T. Nakamura and K. Oohara, Prog. Theor. Phys., **89**, 809 (1993) for simulations of neutron star binary coalescence with and without large plunging velocities.

FIG. 5. The critical orbital frequency (at the inner-most stable orbit) as a function of the ratio of the neutron star radius  $R_o$  and mass  $M$ . The solid curves show the results including both relativistic and tidal effects (the lower curve is for  $\Gamma = 3$  while the upper one is for  $\Gamma = 2$ ), the dashed curves are the Newtonian limit given by Eqs. (8)-(9). The vertical line corresponds to  $R_o/M = 9/4$ , the minimum value for any physical neutron star. The insert is a close-up for the nominal range of  $R_o/M = 4 - 8$  as given by all the available nuclear EOS's. Two curves within the insert should bracket all the physical values of  $f_{\text{isco}}$ .

FIG. 6. The radial infall coordinate velocity during binary coalescence, with  $M = M' = 1.4M_\odot$ ,  $R_o/M = 5$ ,  $\Gamma = 3$ , all calculated using  $2.5PN$  radiation reaction. The solid line is the result including relativistic and tidal effects, the short-dashed line includes only tidal effects, the long-dashed line includes only relativistic effects. The dotted line is the point mass “Newtonian” result.

FIG. 7. The number of orbits the binary spends per logarithmic frequency. The labels are the same as in Fig. 2.

FIG. 8. The quadrupolar gravitational energy emitted near a given frequency. The labels are the same as in Fig. 2.

TABLE I. Physical quantities at the inner-most stable orbit (dynamical stability limit) of neutron star binary, with  $M = M'$ ,  $\Gamma = 3$ , and zero spin at large orbital radii. Here  $R_o$  is the neutron star radius,  $a_1, a_2, a_3$  are the axes of the ellipsoidal neutron star ( $a_1$  along the binary axis,  $a_3$  perpendicular to the orbital plane), and  $M_{1.4} = M/(1.4M_\odot)$ .

The case in the top row is the purely Newtonian calculation using LS equations of motion. The last row is the point-mass calculation using the hybrid equations of motion of KWW.

$R_o/M$	$r/R_o$	$r/M_t$	$a_2/a_1$	$a_3/a_1$	$M_{1.4}f_{orb}(\text{Hz})$
---	2.76	$6.90(R_o/5M)$	.772	.805	$657(5M/R_o)^{3/2}$
8	2.87	11.5	.830	.850	279
6	2.97	8.91	.857	.871	399
5	3.10	7.74	.880	.891	488
4	3.39	6.78	.915	.921	590
0	—	6.03	—	—	697